Astron. Astrophys. 333, 956–969 (1998)

ASTRONOMY AND ASTROPHYSICS

Clumping-corrected mass-loss rates of Wolf-Rayet stars

T. Nugis[1], **P.A. Crowther**[2], **and A.J. Willis**[2]

[1] Tartu Astrophysical Observatory, EE-2444 Tõravere, Estonia
[2] Department of Physics & Astronomy, University College London, Gower Street, London WC1E 6BT, UK

Received 2 September 1997 / Accepted 23 January 1998

Abstract. Mass-loss rates of Galactic Wolf–Rayet stars have been determined from their radio emission power and spectral index ($\alpha = d\ln f_\nu / d\ln \nu$), accounting for the clumped structure and (potential) variable ionization in their outer winds. The average spectral index between mm- and cm- wavelengths is $\sim$0.77 for WN stars and $\sim$0.75 for WC stars, in contrast with $\sim$0.58 expected for smooth winds. The observed wavelength dependence of α can be explained using clumped wind models in some cases, with shocks (at 30–100 stellar radii) producing a higher ionization zone in the outer wind.

We obtain an empirical formula relating mass-loss with observed optical emission line equivalent widths, with application to stars without measured radio fluxes. Clumping-corrected mass-loss rates are generally lower than those obtained by current smooth wind models. Specifically we find $\log \dot{M}$(clumpy)–$\log \dot{M}$(smooth)=-0.19 (σ=0.28) for WN stars, and $\log \dot{M}$(clumpy)–$\log \dot{M}$(smooth)=-0.62 (σ=0.19) for WC stars. New mass-loss rate estimates agree very well with (clumping independent) determinations of WR components in binary systems.

Key words: stars: atmospheres – stars: mass-loss – stars: Wolf-Rayet – radio continuum: stars

1. Introduction

Mass-loss represents one of the most fundamental aspects of hot, luminous stars with important consequences for the mechanical energy and chemical enrichment of heavy elements released into the interstellar medium. The radio continua of hot, massive stars are formed in their outer stellar wind, at typically one thousand stellar radii, where conditions in their winds have reached their asymptotic values, and so provide reliable mass-loss information.

Wolf-Rayet (WR) stars possess the strongest winds of all hot, luminous stars. Centimetre radio emission have been measured for more than 35 WR stars, of which 9 are known to be non-thermal emitters (Abbott et al. 1986; Leitherer et al. 1997). Comprehensive estimates of radio mass-loss rates have been presented by Willis (1991). However, previous estimates of (single) WR stars have been made under the assumption of a smooth outflow, while substantial evidence now exists that their winds are clumped (see e.g. Moffat et al. 1988; Hillier 1991; Robert 1994).

However, do clumps significantly influence line and continuum fluxes, or are they small perturbations giving rise to minor deviations from smooth outflows? Cherepashchuk et al. (1984) found evidence for a great number of relatively small blobs in interpreting the infra-red (IR) eclipse curve of WR 139 (WN5+O 6V), while clumps appeared to play a dominant role in the IR continuum formation of the WR component. The presence of blobs in the optical line emitting region implies lower mass-loss rates than those derived from smooth models (Antokhin et al. 1992; Schmutz 1997). Nugis (1994) has found that IR and radio fluxes observed in WR stars are in conflict with smooth wind predictions. Runacres & Blomme (1996) and Blomme & Runacres (1997) have recently investigated the effect of clumping on the IR and radio continuum of OB stars.

In Sect. 2 of the present paper we will discuss observed IR and radio data of WR stars and determine how spectral indices depend on wavelength. In Sect. 3 we present formulae for obtaining theoretical IR and radio fluxes for smooth and clumped wind models. In Sect. 4 we describe our method for the determination of clumping-corrected "radio" mass-loss rates for WR stars, together with relationships for mass-loss rate estimates obtained from optical emission line strengths. In Sect. 5 we compare mass-loss determinations with other results, and reach our conclusions.

2. Determination of spectral index

2.1. IR and radio observations

Table 1 summarises IR ($\lambda \geq 10\mu$m) and radio fluxes for Galactic WR stars that are probable or definite thermal radio emitters. Leitherer et al. (1997) have recently compiled a list of 9 non-thermal emitters, which are mostly WR + O binaries. In two cases (WR 146, WR 147) thermal WR winds and non-thermal colliding winds have been resolved at radio frequencies, and so are included here (Dougherty et al. 1996; Williams et al. 1997). At quiescence (minimum), the radio emission from WR 140 appears to be thermal.

Send offprint requests to: T. Nugis

Table 1. Observed IR and radio fluxes (in mJy) of Galactic WR stars (ordered by subtype), where extrapolated 12μm values are given in parenthesis (see text). Spectral classifications are from Smith et al. (1996) for WN stars and Smith et al. (1990) for WC stars. In addition to the radio data presented below, there have been detections for WR 134 and WR 11 at 21 cm and 36 cm respectively (WR 134: $f = 0.25 \pm 0.05$–Hogg 1989; WR 11: $f = 8.2 \pm 1.0$–Jones 1985)

WR	Sp.Type	10–12μm ν(GHz)=2.6 10^4	25μm 1.2 10^4	1.2–1.3 mm 2.4 10^2	1.3 cm 23	2 cm 15	3.5 cm 8.6	6 cm 4.9
1	WN4b	550±55 [1]		19±5 [2]			0.47±0.1 [3]	
6	WN4b	890±50 [4]	520±50 [4]	17±3 [2]	2.2±0.5 [5]	2.0±0.3 [5,6]		1.04±0.05[5,6]
133	WN5+O9 I	260±25 [4]		<6 [2]				≤0.3 [7]
138	WN5+B?	340±35 [8]		12±4 [2]				0.6±0.1 [3]
139	WN5+O6 V	460±50 [4]		<8 [2]				0.28±0.08[3]
141	WN5+OB?	(540)		<16 [2]				0.6±0.1 [6]
110	WN5–6b	1180±120[8]		32±6 [2]				0.96±0.1 [3]
24	WN6a	450±50 [9]					1.04±0.09[10]	0.35±0.13[10]
25	WN6a	440±50 [9]					0.90±0.15[10]	
115	WN6	(320)		<14 [2]				0.40±0.09[6]
134	WN6b	580±35 [4]	330±30 [4]	<19 [2]	2.1±0.30[5]	1.97±0.12[5,6]		0.80±0.06[5,6]
136	WN6b	1160±70 [4]	500±95 [4]	29±3 [2]	5.4±0.6 [5]	4.0±0.2 [5,6]		1.95±0.09[5,6]
22	WN7+OB	590±60 [9]					1.50±0.09[10]	1.38±0.13[10]
78	WN7	1100±90 [4]	560±60 [4]	11.6±2.3[11]		3.15±0.35[5,6]		1.50±0.09[5,6]
145	WN7/CE+OB?	550±50 [4]		29±7 [2]	3.0±0.4 [12]	2.4±0.13[6]		0.98±0.15[3]
16	WN8	490±30 [4]	390±55 [4]				1.75±0.09[10]	1.21±0.09[10]
40	WN8	640±60 [4]	310±40 [4]				2.52±0.09[10]	1.69±0.10[10]
89	WN8+abs	(490)					2.99±0.10[10]	1.94±0.19[10]
							0.60±0.14[6]	
98	WN8/C7	(240)		19±5 [2]				0.90±0.07[6]
147	WN8+OB	5640±340[4]	2850±290[4]	379±55 [2]	49.4±5.0 [13]	35.6±5.0 [13]		20.4±1.0 [13]
144	WC4	(330)		<25 [2]				0.67±0.25[3]
9	WC5+O7	(420)		<25 [2]				0.67±0.25[3]
111	WC5	340: [8,14]		<21 [2]				0.33±0.1 [3]
15	WC6	550±50 [4]					0.69±0.11[15]	<0.33 [15]
146	WC6+O	910±300[4]		30±9 [16]				1.0±0.2 [16]
79	WC7+O5-8	920±90 [9]				2.0±0.4 [5]		1.12±0.08[5,6]
86	WC7+B0 I	(470)						0.50±0.07[6]
93	WC7+O7-9	(940)						0.90±0.2 [6]
137	WC7+OB	580±60 [17]	290±30 [17]	<10 [2]				0.37±0.08[3]
140	WC7+O4-5	1360±90 [18]	640±130[18]	23±3 [2]		3.3±0.2 [19]		1.25±0.1 [19]
11	WC8+O9	13900±600[4]	6760±350[4]	342±27 [11]		67±5 [20]	32.2±0.63[15]	26.5±0.28[15]
113	WC8+O8-9 IV	(530)					<0.80 [15]	≤0.40 [3]
135	WC8	380±40 [8]		<52 [2]				0.60±0.09[7]
65	WC9	(480)					0.37±0.14[15]	<0.42 [15]
81	WC9	(440)						0.30±0.08[6]
103	WC9	(250)					<0.42 [15]	≤0.20 [6]
112	WC9	(1300)					0.68±0.13[15]	<0.39 [15]

[1]-Hackwell et al. 1974, [2]-Altenhoff et al. 1994, [3]-Bieging et al. 1982, [4]-IRAS data, [5]-Hogg 1989, [6]-Abbott et al. 1986, [7]-Hogg 1982, [8]-Cohen et al. 1975, [9]-Barlow et al. 1981, [10]-Leitherer et al. 1995, [11]-Leitherer & Robert 1991, [12]-Felli & Panagia 1982, [13]-Churchwell et al. 1992, [14]-Hillier 1989, [15]-Leitherer et al. 1997, [16]-Dougherty et al. 1996, [17]-Williams et al. 1985, [18]-Williams et al. 1990, [19]-Becker & White 1985, [20]-Morton & Wright 1978

For those WR stars not observed at mid-IR wavelengths or contaminated by dust emission at that range, we have extrapolated near-IR or visible fluxes to 12μm (shown in parenthesis), assuming their spectral index is identical to the dust-free stars of similar subclasses. Near-IR photometry was taken from Hackwell et al. (1974), Cohen et al. (1975), Williams & Antonopoulou (1981), Pitault et al. (1983), Williams et al. (1987) and Crowther et al. (1995b). Line contributions in the near-IR bands were estimated from Pitault et al. (1983). The IR emission from WR 140 and WR 137 appear to be uncontaminated by dust emission during quiescence (minimum).

2.2. Distances and interstellar reddenings

Before we can obtain mass-loss rate estimates for our programme WR stars it is necessary to obtain distances, and interstellar reddening estimates to transform observed continuum fluxes into de-reddened fluxes.

Interstellar reddenings, E_{B-V}, are given in Table 2. Our assumed reddening is taken from the mean of (i) literature values obtained by nulling the λ2200 interstellar feature (Morris et al. 1993, Crowther 1993, Vacca & Torres-Dodgen 1990, Ford & Stickland 1988, Garmany et al. 1984, Underhill 1983, Nussbaumer et al. 1982, Hamann & Schwarz 1992, Eaton et al. 1985 and Stickland et al. 1984), and (ii) intrinsic colours, taken from Nugis & Niedzielski (1995) for single WR stars and from companion–corrected intrinsic colours for binary WR stars. The relationship between E_{B-V} and monochromatic colour excess E_{b-v} is adopted from Schmutz & Vacca (1991): $E_{B-V} = 1.24E_{b-v}$ ($A_V = 3.1E_{B-V}$). Turner (1982) derived a slightly different relationship: $E_{B-V} = 1.21E_{b-v}$. In order to correct intrinsic colours for binarity, we adopted $(b-v)_0$=−0.35 for O stars and −0.30 for B companions (the latter value is also used for the companions classified as "abs") following Massey (1984). For several stars we deviated from the above technique:

- WR 25 lies in a region of peculiar UV interstellar extinction (Crowther et al. 1995a), for which we obtained $E_{B-V} = 0.73$ by demanding identical $f_\nu(\mathrm{v})/f_\nu(\mathrm{K})$ and $f_\nu(\mathrm{v})/f_\nu(\mathrm{N})$ ratios to WR 24 which has an identical spectral type.
- For WR 147 we determined E_{B-V} from $f_\nu(\mathrm{v})/\mathrm{f}_\nu(\mathrm{K})$ relative to normal WN8 stars and that obtained by Stickland et al. (1984).
- Since no reliable estimate of $(b-v)$ exists for WR 144 we have obtained its reddening assuming an identical intrinsic $(r-v)$ colour to WR 111 (WC5).

Distances, as presented in Table 2, have been derived using various techniques. For those stars which are not thought to be members of an open cluster or association, we generally used the mean absolute visual magnitudes for the respective WR (or O) spectral subtype. For most WN subtypes we obtained absolute visual magnitudes from members of clusters/associations, while we follow van der Hucht et al. (1988) for WC stars. For WR 6 and WR 124 we adopt distances obtained from their interstellar line spectra (Howarth & Schmutz 1995; Crawford & Barlow 1991). Distances to open clusters or associations are taken from Lundström & Stenholm (1984) and van der Hucht et al. (1988). For WR 78, WR 79 and WR 133 we use improved distances from Smith et al. (1994). Other exceptions are:

- WR 11 (WC8+O9 III) – Schaerer et al. (1997) reported the HIPPARCOS parallax measurements for this binary and derived a significantly smaller distance (0.26±0.04 kpc) than previously assumed (0.45 kpc).
- WR 47 (WN6+O5 V) – this star is normally assumed to be a member of the open cluster Ho 15 with a distance of 3.80 kpc. However, with this distance we obtain that $M_v^{\mathrm{O}} = -4.81$, which is far from the mean of −5.43 for O5 V stars (Vacca et al. 1996). Smith et al. (1994) obtained a mass for the WN6 component which is much lower than that obtained from the orbital study of Moffat et al. (1990) – $M_{\mathrm{W}} \leq 10M_\odot$ instead of $\approx 48M_\odot$. An improved consistency is obtained using a revised distance of 4.30 kpc, obtained by requiring identical differences in absolute visual magnitudes relative to mean values for their spectral types.
- WR 139 (WN5+O6 V) – both components are unusually bright ($M_v^{\mathrm{W}} = -4.97$ and $M_v^{\mathrm{O}} = -5.64$) on the assumption that it is a member of the open cluster Be 86 ($d \approx 1.74$ kpc, Nugis 1996). A revised distance was estimated from the radius of the O component obtained by St-Louis et al. (1993). With R_{O}=8.5±1 $R_\odot$, $E_{B-V} = 0.88$, L_{O}=0.65 and using $T_{\mathrm{eff}}(\mathrm{O6V})$=43 560 K and BC=−4.06 (Vacca et al. 1996), we find a distance of d=1.13±0.15 kpc.

For binaries, we have determined the fraction of the total light emitted by the WR component in the v-band (L_{W}) using the strength of (helium, nitrogen/carbon) WR emission (L_{em}) and OB absorption (L_{abs}) lines relative to single stars and absolute visual magnitudes of the components. Smith et al. (1996) derived a relationship between W_λ(He II λ5411) and FWHM(He II λ4686) allowing estimates to be made of the fractional continuum brightness of WN components in binaries. For WC binaries we compared emission lines of $\lambda\lambda$ 5806, 5696, 5590, 5470, 5411 relative to single Galactic stars.

2.3. Stellar abundances and wind velocities

Determinations of mass-loss rates from radio observations require knowledge about wind velocities and chemistries. In general, wind velocities are taken from UV P Cygni resonance lines (Prinja et al. 1990, Rochowicz & Niedzielski 1995), or near-IR He I P Cygni profiles (Eenens & Williams 1994) and are listed in Table 2 (see footnotes for exceptions).

For chemical compositions we consider the three most abundant elements in atmospheres under consideration; H, He and N for WN stars and He, C, O for WC stars. The contribution of other elements does not affect mean molecular weights. Hydrogen-to-helium ratios presented for WN stars are obtained from clumped models of Nugis & Niedzielski (1995), or smooth models of Hamann et al. (1995) and Crowther et al. (1995a,b) if these were unavailable. N/He abundances are set to 0.005 for WN stars following estimates from Nugis (1991) and Crowther (1993). Throughout this paper, abundance ratios are presented by number. The chemical composition of the star WR 145 (WN7/CE+OB) is taken from Crowther et al. (1995c) and the composition of the star WR 98 (WN8/C7) is adopted to be the same as for WR 145. In the case of WC stars, we take C/He=0.5 for WC4–5 stars, 0.4 for WC6 stars, 0.3 for WC7 stars, 0.2 for WC8 stars and 0.1 for WC9 stars, and O/C=0.1 following Nugis (1991).

The ionic charge (numbers of valence electrons z_n^{asym}), number of electrons per ion and asymptotic value of the electron temperature (T_e^{asym}) depend on the ionization conditions

Table 2. Physical parameters of WR stars with detected thermal radio-emission. Monochromatic magnitudes, m_v, were generally taken from Torres-Dodgen & Massey (1988) or from Massey (1984). For those stars without monochromatic magnitudes, we corrected synthetic magnitudes by -0.04 mag (Schmutz & Vacca 1991) for WN stars, or -0.06 mag for WC stars (our estimate). $L_{\rm W}$ is the fraction of the total flux emitted by the WR component in the v-band. The method of distance estimate is given in parenthesis: (a) - member of an association/cluster, (IS) - IS line study, (M_v) - fixed absolute visual magnitude, ($R_{\rm O}$) - fixed radius, (par) - parallax measurement. The asymptotic valence electrons correspond to the normal (n) clumped wind case (z_n(He)=1 for all our sample). For the higher ionization zones we assume $z_h({\rm He}) = 2$, $z_h({\rm N}) = {\rm z_n(N)} + 1$, $z_h({\rm C}) = 4$ for WN stars and $z_h({\rm C}) = 4$, $z_h({\rm O}) = 5$ for WC stars

WR	m_v	$(b-v)_0$	d		E_{B-V}	$L_{\rm W}$	$M_v^{\rm W}$	v_∞	H/He	$T_e^{\rm asym}$	z_n(C)	z_n(N)	z_n(O)
	mag	mag	kpc		mag		mag	km s^{-1}		K			
1	10.54	−0.15	2.63	(a)	0.85	1.0	−4.47	2 135 (13)	0.1	15 000	3	3	...
6	6.96	−0.15	1.80	(IS)	0.06	1.0	−4.52	1 720 (14)	0.2	15 000	3	3	...
133	6.70	−0.25	1.66	(a)	0.38	0.12 (1)	−3.40	1 625 (14)	0.0	15 000	3	3	...
138	8.11	−0.25	1.82	(a)	0.65	0.41 (2)	−4.45	1 345 (14)	0.8	15 000	3	3	...
139	8.10	−0.25	1.13	($R_{\rm O}$)	0.88	0.35 (3)	−4.04	1 785 (14)	0.2	15 000	3	3	...
141	10.14	−0.25	1.82	(a)	1.14	0.70 (2)	−4.67	1 400 (15)	0.0	15 000	3	3	...
110	10.26	−0.10	1.76	($M_v^{\rm W}$)	1.15	1.0	−4.90	2 300 (15)	0.0	14 000	3	3	...
24	6.50	−0.20	2.63	(a)	0.18	1.0	−6.22	2 155 (14)	2.4	13 000	3	3	...
25	8.18	−0.20	2.63	(a)	0.73 (11)	1.0	−6.42	2 455 (14)	3.8	13 000	3	3	...
115	12.35	−0.20	2.19	(a)	1.61	1.0	−4.86	1 150 (15)	0.0	13 000	3	3	...
134	8.24	−0.10	2.09	(a)	0.46	1.0	−4.93	1 905 (14)	0.2	13 000	3	3	...
136	7.64	−0.10	1.82	(a)	0.54	1.0	−5.51	1 605 (14)	0.5	13 000	3	3	...
22	6.45	−0.20	2.63	(a)	0.32	0.90 (4)	−6.63	1 790 (14)	3.2	11 000	3	3	...
78	6.62	−0.20	1.58	(a)	0.51	1.0	−6.12	1 365 (14)	0.4	11 000	3	3	...
145	12.54	−0.20	1.82	(a)	2.05 (5)	0.40 (5)	−4.78	1 390 (5)	0.0	11 000	3	3	...
16	8.52	−0.15	3.42	($M_v^{\rm W}$)	0.57	1.0	−6.10	740 (14)	1.8	10 000	2	2	...
40	7.87	−0.15	3.11	($M_v^{\rm W}$)	0.44	1.0	−6.10	910 (14)	0.8	10 000	2	2	...
89	11.55	−0.15	2.88	(a)	1.80	0.40 (2)	−5.91	1 500 (16)	1.0	10 000	2	2	...
98	12.53	−0.15	2.47	($M_v^{\rm W}$)	1.57	1.0	−4.80	1 150 (15)	0.0	10 000	2	2	...
147	14.89	−0.15	0.62	($M_v^{\rm W}$)	3.65 (11)	0.65 (2)	−6.10	900 (17)	0.1	10 000	2	2	...
144	15.45	−0.32	1.12	($M_v^{\rm W}$)	2.40 (11)	1.0	−3.00	2 440 (16)	...	10 000	3	...	4
9	11.01	−0.32	2.06	($M_v^{\rm O}$)	1.46	0.41 (2)	−4.58	3 030 (18)	...	9 000	3	...	4
111	8.41	−0.32	1.58	(a)	0.30	1.0	−3.61	2 415 (14)	...	9 000	3	...	4
15	11.85	−0.32	1.44	($M_v^{\rm W}$)	1.39	1.0	−3.70	2 325 (13)	...	8 500	3	...	4
146	13.91	−0.32	0.70	($M_v^{\rm W}$)	2.80 (6)	0.33 (6)	−3.70	2 700 (6)	...	8 500	3	...	4
79	6.97	−0.30	1.58	(a)	0.48	0.45 (2)	−4.80	2 270 (14)	...	8 000	2	...	3
86	9.72	−0.30	2.16	($M_v^{\rm W}$)	0.99	0.61 (7)	−4.80	1 800 (15)	...	8 000	2	...	3
93	11.52	−0.30	1.74	(a)	1.82	0.47 (2)	−5.09	2 290 (14)	...	8 000	2	...	3
137	8.21	−0.30	1.82	(a)	0.66	0.60 (8)	−4.80	1 885 (14)	...	8 000	2	...	3
140	7.10	−0.30	1.21	($M_v^{\rm O}$)	0.84	0.45 (6)	−5.32	2 800 (15)	...	8 000	2	...	3
11	1.78	−0.30	0.26	(par)	0.03	0.15 (9)	−3.34	1 415 (14)	...	7 500	2	...	3
113	9.48	−0.30	2.00	(a)	1.02	0.50 (10)	−4.76	1 890 (14)	...	7 500	2	...	3
135	8.50	−0.30	2.09	(a)	0.38	1.0	−4.40	1 405 (14)	...	7 500	2	...	3
65	14.61	−0.25	2.13	($M_v^{\rm W}$)	2.27	1.0	−4.80	1 040 (16)	...	7 000	2	...	2
81	12.99	−0.25	2.23	($M_v^{\rm W}$)	1.77	1.0	−4.80	900 (15)	...	7 000	2	...	2
103	9.18	−0.25	2.94	($M_v^{\rm W}$)	0.48	1.0	−4.80	1 190 (14)	...	7 000	2	...	2
112	19.1:	−0.25	1.30	($M_v^{\rm W}$)	3.90 (12)	1.0	−4.80	1 100 (19)	...	7 000	2	...	2

(1)-Smith & Maeder (1989), (2)-$L_{\rm em}$, (3)-the mean of $L_{\rm abs}$ (Cherepashchuk et al. 1995) and $L_{\rm em}$, (4)-Rauw et al. (1996), (5)-Crowther et al. (1995c), (6)-Willis et al. (1997), (7)-ΔM_v, (8)-$M_v^{\rm W} = -4.8$, (9)-the mean of $L_{\rm abs}$ (Smith & Maeder 1989) and L_{M_v} ($M_v^{\rm O} = -5.28$, Schaerer et al. 1997), (10)-Massey & Niemela (1981), (11)-see text, (12)-Williams et al. (1987), (13)-Rochowicz & Niedzielski (1995), (14)-Prinja et al. (1990), (15)-Eenens & Williams (1994), (16)-v_∞=0.74 v(Abbott et al. 1986/Torres 1985), as derived by Willis (1991), (17)-Churchwell et al. (1992), (18)-v_∞ (WC5)≈43.9 FWHM (C IV λ5801-12), derived us from observations of Smith et al. (1990), (19)-the mean for WC9 stars

in the outer wind. For smooth winds, the ionic charge is readily obtained from the lowest observed ionization state in optical subordinate lines (e.g. $z_n^{\rm asym}$(He)=1 if He I is observed in the spectrum). Estimates for individual stars are given in Table 2 for the clumped case – where either no interaction takes place between clumps or this is too weak to cause additional ionization in the radio emitting region.

Table 3. Observed spectral indices ($\alpha_{\lambda(1)-\lambda(2)} = \ln(f_{\nu_1}/f_{\nu_2})/\ln(\nu_1/\nu_2)$) for those WR stars which have been observed at least two radio frequencies. Radio "maximum" fluxes have been used for WR 89, while spectral indices derived from extrapolated IR fluxes are given in parenthesis

WR	$\alpha_{12\mu m-6cm}$	$\alpha_{12\mu m-25\mu m}$	$\alpha_{12\mu m-1.2mm}$	$\alpha_{25\mu m-1.2mm}$	$\alpha_{1.2mm-2/3.5cm}$	$\alpha_{1.2mm-6cm}$	$\alpha_{2/3.5cm-6cm}$	$\alpha_{6cm-21/36cm}$
1	0.88±0.04		0.71±0.08			0.94±0.12		
6	0.79±0.01	0.73±0.20	0.86±0.05	0.89±0.07	0.76±0.12	0.71±0.05	0.59±0.18	
138	0.74±0.03		0.71±0.10			0.76±0.13		
110	0.83±0.03		0.76±0.06			0.89±0.08		
24	0.83±0.06					1.85±0.80		
134	0.77±0.02	0.77±0.20	>0.74	>0.74	<0.81	<0.81	0.81±0.12	0.96±0.22
136	0.75±0.02	1.15±0.35	0.80±0.04	0.74±0.08	0.70±0.06	0.69±0.04	0.64±0.08	
22	0.71±0.02						0.14±0.26	
78	0.78±0.02	0.92±0.26	0.97±0.06	0.98±0.08	0.48±0.12	0.53±0.07	0.66±0.15	
145	0.74±0.03		0.64±0.07		0.88±0.11	0.86±0.10	0.81±0.18	
16	0.70±0.02	0.31±0.30					0.63±0.22	
40	0.69±0.02	0.99±0.30					0.68±0.16	
89	(0.65)						0.74±0.22	
98	(0.65)		(0.55)			0.78±0.09		
147	0.66±0.01	0.93±0.22	0.59±0.04	0.52±0.06	0.74±0.05	0.84±0.10	0.49±0.17	
146	0.79±0.06		0.76±0.14			0.85±0.13		
79	0.78±0.02						0.52±0.24	
140	0.82±0.02	1.45±0.55	0.89±0.04	0.82±0.08	0.69±0.07	0.74±0.055	0.88±0.12	
11	0.73±0.01	0.98±0.13	0.79±0.03	0.76±0.04	0.59/0.72	0.66±0.03	0.83/0.33	0.67±0.08

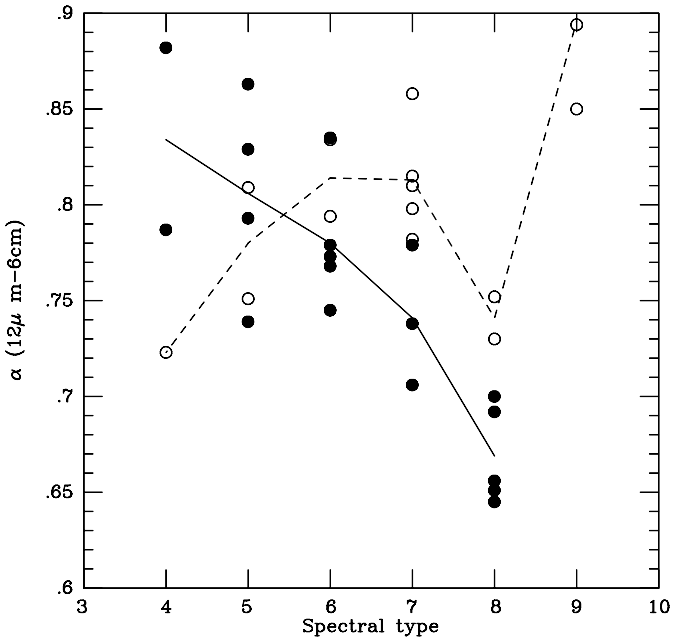

Fig. 1. The dependence of the 12μm–6cm spectral index with spectral subtype for individual WN (filled) and WC (open) stars. The decrease in mean spectral index at later WN spectral types (solid) is not repeated for WC stars (dashed)

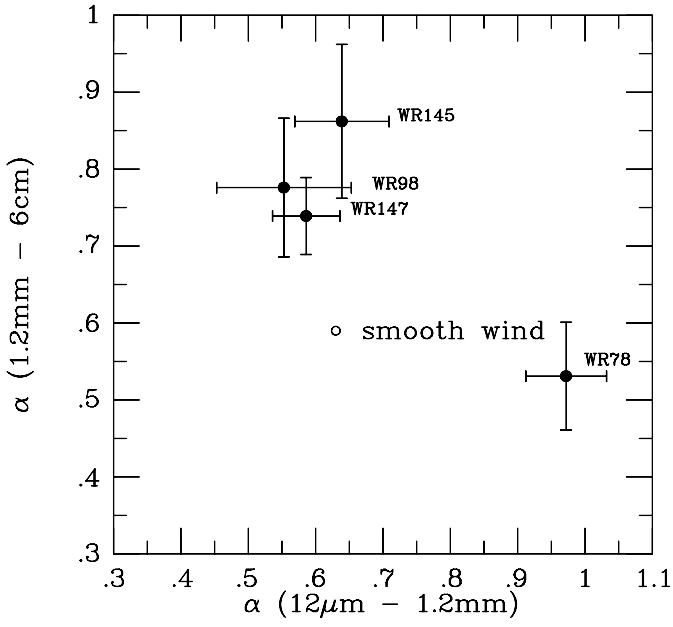

Fig. 2. The spectral indices $\alpha_{1.2mm-6cm}$ versus $\alpha_{12\mu m-1.2mm}$ for WN7–8 stars which indicate a complicated structure of clumped WNL winds (an open circle corresponds to the predictions of the smooth WNL wind model)

2.4. Spectral indices

We now turn to the IR-mm-cm spectral indices ($\alpha = d\ln f_\nu / d\ln\nu$) for our program stars, using the fluxes tabulated in Table 1. Individual values between IR–mm and mm–cm wavelengths are presented in Table 3 for those stars with two measurements at mm–cm wavelengths. We find spectral indices ∼0.9–1.1 in the IR spectral range, tending towards 0.6 at centimetre wavelengths.

Table 4. Comparison between observed IR–mm–cm spectral indices for WR 78 (WN7) with predictions from the asymptotic smooth wind model, a clumped wind model (Model I) with clumps dominating the formation of IR and radio fluxes in the whole range and a clumped wind model (Model II) with clumps dominating the formation of IR and mm-fluxes, and an enhancement factor due to clumping approaching unity in the region where cm fluxes are formed. Two different solutions are presented for Model II with a normal ionization structure ("n") and with a higher ionization status in the far wind ("nhn"). Smooth wind and clumped wind Model I are in conflict with observations

α	obs.	sm. asym	clumped I	clumped II 'n'	clumped II 'nhn'
12μm −25μm	0.92±0.26	0.50	0.87	0.85	0.84
25μm −1.3mm	0.98±0.08:	0.55	0.91	0.86	0.84
1.3mm−2cm	0.48±0.12:	0.58	0.93	0.64	0.67
2cm −6cm	0.66±0.15	0.59	0.94	0.59	0.67
12μm −6cm	0.78±0.02	0.56	0.92	0.75	0.76

The average spectral index between IR and centimetre wavelengths is ∼0.75 ($0.65 \leq \alpha_{\rm IR-cm} \leq 0.87$) for 20 WN stars and a trend towards lower values at later spectral type (see Fig. 1). In the case of WC stars the derived spectral index between IR and cm wavelengths is 0.82 ($0.73 \leq \alpha_{\rm IR-cm} \leq 0.95$) for 17 stars, with no clear trend to lower values at later WC subtypes.

For those WR stars also observed at millimetre wavelengths, the average spectral index between mm–cm wavelengths is 0.77 for 9 WN stars (0.53–0.94) and 0.75 for 3 WC stars (0.66–0.85). Observed spectral indices over the IR–mm–cm range show substantial variations, even amongst similar spectral types as illustrated by WN7–8 stars in Fig. 2. In cases where dust contaminates IR fluxes (e.g. WC9 stars, Williams et al. 1987), we have restricted our study to the use of extrapolated fluxes.

3. IR and radio continuum formation in a smooth or clumpy wind

In this section we describe the determination of formulae used to derive radio mass-loss rates, following the numerical technique, assumptions and nomenclature of Nugis (1990) adapted for clumpy winds by Nugis & Niedzielski (1995) to which the reader is referred for a detailed description. As usual, we adhere to spherical symmetry throughout.

3.1. Smooth wind solution

Continuum fluxes at IR ($\lambda \geq 10\mu$m) and radio wavelengths were found iteratively by direct numerical integration of Eqs. (42–44) in Nugis & Niedzielski (1995). At IR and radio wavelengths, the absorption coefficient is dominated by free-free transitions, with small bound-free contributions at IR wavelengths, and electron scattering unimportant (Nugis 1994, Nugis & Niedzielski 1995).

The transfer of radiation in the outer stellar winds of hot stars was considered by Panagia & Felli (1975) and Wright & Barlow (1975), assuming asymptotic values of temperature, wind velocity, a constant ionization state and smooth outflow. With these assumptions, the intensity $I_\nu(\xi)$ at a radio wavelength from any line-of-sight with $\xi \gg R_*$ (R_* is the stellar radius, and ξ is the impact parameter) is given by

$$I_\nu(\xi) = B_\nu(1 - e^{-\tau_\nu(\xi)}), \tag{1}$$

where the optical depth $\tau_\nu(\xi)$ is

$$\tau_\nu(\xi) = \frac{2\dot{M}^2\gamma\zeta k_\nu^\circ}{(4\pi\mu m_u v_\infty)^2}\int_\xi^\infty \frac{dr}{r^3\sqrt{r^2-\xi^2}} = \\ = \frac{\dot{M}^2\gamma\zeta k_\nu^\circ}{(4\pi\mu m_u v_\infty)^2}\frac{\pi}{2\xi^3}, \tag{2}$$

where $\dot{M}$ is the mass-loss rate, m_u is the atomic unit mass, μ is the mean atomic weight, γ is the mean number of electrons per atom, and k_ν° is given by Eq. (45) in the paper of Nugis & Niedzielski (1995). ζ is given by

$$\zeta = \sum_{A,z} x^+ z^2 (g_{ff} + \frac{2z^2 I_H}{kT_e}\sum_{i=k}^{\infty}\frac{g_{i\nu}}{i^3}e^{\frac{I_i}{kT_e}}), \tag{3}$$
$$\frac{I_k}{h} < \nu < \frac{I_{k-1}}{h}, \quad x^+ = N_A^{+z}/N_t.$$

Here N_A^{+z} is the number of z-times ionized atoms of the element A, N_t is the total number of atoms of all elements, I_i is the ionization energy of level i of $z-1$ times ionized atoms of the element A and g_{ff} and $g_{i\nu}$ are the Gaunt factors for free–free and bound–free transitions. Free-free Gaunt factors at long wavelengths ($u = h\nu/kT < 10^{-4}$) can be precisely found through the Spitzer formula:

$$g_{ff} = \frac{\sqrt{3}}{\pi}\Big(17.72 + \ln\frac{T_e^{1.5}}{z\nu}\Big). \tag{4}$$

At wavelengths with $u = h\nu/kT \geq 10^{-4}$ the free-free Gaunt factors can be found by interpolation from the Tables of Carson (1988).

To obtain the total emission, we must integrate the intensity, $I_\nu(\xi)$, along a line-of-sight over the entire wind and multiply by 4π to account for the isotropy of the emission. Thus we have:

$$4\pi d^2 f_\nu = 4\pi\int_0^\infty B_\nu(1 - e^{-\tau_\nu(\xi)})2\pi\xi d\xi, \tag{5}$$

where f_ν is the observed, de-reddened flux. Following Panagia & Felli (1975) we can divide this into two parts (the first part corresponds to the optically thick zone with small impact parameters ξ):

$$d^2 f_\nu = \pi B_\nu\Big(C(\tau_c)\int_0^{\xi_c} 2\xi d\xi + \int_{\xi_c}^\infty 2\xi(1 - e^{-\tau_\nu(\xi)})d\xi\Big). \tag{6}$$

If to choose ξ_c so that $\tau_c = \tau_\nu(\xi_c)$ is much higher than unity, then $C(\tau_c) = 1.0$. For numerical calculations it is enough to use ξ_c so that $\tau_\nu(\xi_c) = 3$ ($C(\tau_c = 3) = 0.9924$). The first integral in parenthesis is equal to $C(\tau_c)\xi_c^2$ and the second integral can be expanded into:

$$\int_{\xi_c}^\infty 2\xi(1 - e^{-\tau_\nu(\xi)})d\xi = 2\xi_c^2\langle\tau_c\rangle, \tag{7}$$

where

$$\langle\tau_c\rangle = \sum_{n=1}^{\infty} \frac{(-1)^{n+1}\tau_c^n}{n!(3n-2)}. \quad (8)$$

Therefore the observed flux becomes:

$$f_\nu = \frac{\pi B_\nu \xi_c^2}{d^2}\Big(C(\tau_c) + 2\langle\tau_c\rangle\Big). \quad (9)$$

From this formula and the formula for τ (Eq. 2), we can write down the smooth wind mass-loss rate as follows

$$\dot{M} = c_1 \frac{f_\nu^{0.75} d^{1.5} \mu v_\infty}{(\nu\gamma\zeta)^{0.5}} \frac{(e^{h\nu/kT_e}-1)^{0.25}\sqrt{e^{h\nu/kT_e}}}{(h\nu/kT_e)^{0.25}}, \quad (10)$$

where c_1 is a numerical constant. As τ_c increases, the ratio $\tau_c^{0.5}/[C(\tau_c)+2\langle\tau_c\rangle]^{0.75}$ quickly approaches an asymptotic value of 0.478. We obtain the mass-loss rate

$$\dot{M} = 0.0938 \frac{f_\nu^{0.75} d^{1.5} \mu v_\infty}{\nu^{0.5}\gamma^{0.5}\zeta^{0.5}} \frac{(e^{h\nu/kT_e}-1)^{0.25}\sqrt{e^{h\nu/kT_e}}}{(h\nu/kT_e)^{0.25}} \quad (11)$$

using the usual units for mass-loss rate ($M_\odot$ yr^{-1}), distance (kpc), terminal velocity (km s^{-1}), flux (Jy) and frequency (Hz). At IR and radio wavelengths $h\nu/kT_e \ll 1$, so the term involving T_e tends towards unity. For an asymptotic smooth wind, the continuum fluxes depend on frequency as follows:

$$f_\nu \propto (\gamma\zeta\nu)^{2/3} \frac{(h\nu/kT_e)^{1/3}}{(e^{h\nu/kT_e}-1)^{1/3}(e^{h\nu/kT_e})^{2/3}}. \quad (12)$$

We can now calculate spectral indices for individual stars. Table 4 compares observations of WR 78 (WN7) with predicted indices, demonstrating the poor agreement achieved for a smooth wind. Even if we assume that helium is doubly ionized where the 12μm continuum flux is formed and singly ionized in the radio-emission zone, the predicted 12μm-6cm index of 0.68 still differs from the observed index of 0.77.

At this stage we should highlight one limitation with our analysis. We assume that the entire IR–radio continuum flux is formed in the asymptotic regime, where the wind velocity, temperature and ionization structure have reached their final values. In WR stars, this regime is not reached at mid-IR wavelengths. Consequently this model underestimates the IR–radio spectral index α by about 0.05–0.10 (early-type WR stars) or 0.02-0.06 (late-type WR stars). Therefore, longer wavelength indices ($\lambda \geq 0.3$mm) provide a more reliable indicator. Nevertheless, serious discrepancies remain for all WR stars under investigation assuming a smooth outflow.

3.2. Clumped wind solution - constant filling factor and density contrast

We now turn to the derivation of the observed continuum flux for a clumped wind. From the equation of mass continuity (see also Nugis & Niedzielski 1995):

$$\dot{M} = 4\pi r^2 \mu v m_u [N^l p\delta + N^l(1-\delta)] = const. \quad (13)$$

The enhancement of continuum emission in the radio spectral region has been derived by Abbott et al. (1981) and Lamers & Waters (1984). They assumed that δ (the filling factor), and p (the density contrast) are *constant* with radial distance. In addition, we assume that clumps have the same T_e and ionization state as interclump material, which should be reasonable provided matter is not predominantly neutral, and no substantial interactions take place in the wind.

The optical depth along a particular line-of-sight can be found from

$$\begin{aligned}\tau_\nu(\xi) &= \frac{2\dot{M}^2\gamma\zeta k_\nu^\circ}{(4\pi\mu m_u v_\infty)^2}\int_\xi^\infty \frac{EF dr}{r^3\sqrt{r^2-\xi^2}} \quad (14)\\ &= \frac{\dot{M}^2\gamma\zeta k_\nu^\circ}{(4\pi\mu m_u v_\infty)^2}\frac{EF\pi}{2\xi^3},\end{aligned}$$

which is identical to the smooth case (Eq. 2) except for an enhancement factor EF:

$$EF = \frac{(p^2\delta + 1 - \delta)}{(p\delta + 1 - \delta)^2}. \quad (15)$$

In the case of a constant EF we obtain an identical relationship for the mass-loss rate as Eq. (11) except for $(EF)^{0.5}$ in the denominator. Equally, the continuum flux has an identical form to the smooth case (Eq. 12) except for a $(EF)^{2/3}$ factor. Therefore, the IR-radio spectral index α is identical to the smooth wind case, and so fails to explain the observed spectral indices. *We therefore have to relax the assumption that clumping is constant throughout the wind.*

3.3. Clumped wind solution – variable filling factor and density contrast

Antokhin et al. (1992), Nugis (1994) and Nugis & Niedzielski (1995) have studied conservative clumped wind models, in which clumps yield variable filling factors and density contrasts with radial distance. The matter density of the clumps is determined by their expansion rate which is close to the local sound speed (Eq. (46) of Nugis & Niedzielski 1995). Clumps are assumed to be uniform, spherical, formed at the stellar surface and move with an identical T_e and velocity law (β of unity) as the interclump medium. EF is around unity near the stellar surface, increasing to a maximum at $\sim$5–10 R_*, and subsequently returning to unity in the outer wind. The precise value of the enhancement factor depends on the inner matter contrast, filling factor and the mean size of clumps at the stellar surface.

Since we are interested in deriving mass-loss rates from radio fluxes in the present work we do not need to consider the precise inner wind structure, and instead develop equivalent relationships to the smooth case described earlier. We consider the wind from where EF reaches its maximum value up to the radius, $r_{\rm asym}$, at which EF returns to unity, where the filling factor reaches its maximum value $\delta_{\rm asym}$ and p=1. In the asymptotic region the clumped volume behaves linearly with radius ($\delta = \delta_{\rm asym} r/r_{\rm asym}$). Incorporating the functional form of the

enhancement factor into the optical depth relation along a particular line-of-sight (Eq. 14) we find

$$\tau_\nu(\xi) =$$

$$\frac{\dot{M}^2 k_\nu^\circ}{(4\pi\mu m_u v_\infty)^2}\left(\int_\xi^{r_{\rm asym}} \frac{\gamma\zeta\delta_{\rm asym} r_{\rm asym} dr}{r^4\sqrt{r^2-\xi^2}}\right.$$

$$\left. + \int_\xi^{r_{\rm asym}} \frac{\gamma\zeta(1-\delta_{\rm asym})^2 dr}{r^3(1-\delta)\sqrt{r^2-\xi^2}} + \int_{r_{\rm asym}}^\infty \frac{\gamma\zeta dr}{r^3\sqrt{r^2-\xi^2}}\right). \quad (16)$$

The observed flux then follows from

$$f_\nu = \frac{\pi B_\nu}{d^2}\left(\xi_c^2 + \int_{\xi_c}^{r_{\rm asym}} (1-e^{-\tau_\nu}) 2\xi d\xi + 2r_{\rm asym}^2 \langle\tau_{r_{\rm asym}}\rangle\right), \quad (17)$$

where ξ_c is such that $\tau_\nu(\xi_c) \geq 3$. Assuming clumps dominate the IR and radio continuum formation, the leading integral term in Eq. (16) becomes dominant so that:

$$\tau_\nu(\xi) \;=\; \frac{\dot{M}^2 k_\nu^\circ \gamma\zeta\delta_{\rm asym} r_{\rm asym}}{(4\pi\mu m_u v_\infty)^2}\frac{4}{3\xi^4}.$$

In this case, the observed flux is

$$f_\nu \;=\; \frac{\pi B_\nu \xi_c^2}{d^2}\Big(1 + 2\langle\langle\tau_c\rangle\rangle\Big) = \quad (18)$$

$$= \frac{c_2 \nu \dot{M}}{d^2 v_\infty \mu}\frac{(\gamma\zeta\delta_{\rm asym} r_{\rm asym})^{0.5} T^{0.25} (h\nu/kT_e)^{0.5}}{[(e^{h\nu/kT_e}-1)e^{h\nu/kT_e}]^{0.5}},$$

where c_2 is a numerical constant and

$$\langle\langle\tau_c\rangle\rangle = \sum_{n=1}^{\infty} \frac{(-1)^{n+1}\tau_c^n}{n!(4n-2)}. \quad (19)$$

Finally, the mass-loss rate is:

$$\dot{M} = c_3 \frac{f_\nu d^2 v_\infty \mu [(e^{h\nu/kT_e}-1)e^{h\nu/kT_e}]^{0.5}}{\nu(\gamma\zeta\delta_{\rm asym} r_{\rm asym})^{0.5}(h\nu/kT_e)^{0.5} T_e^{0.25}}, \quad (20)$$

where c_3 is a numerical constant.

Substantially higher IR-radio spectral indices result relative to a smooth wind case, as illustrated in Table 4 for WR 78 (clumped wind Model I). However, from the observed spectral indices, clumps do not appear to dominate the *entire* IR-radio continuum formation. Observations can only be reproduced if clumps dominate at IR wavelengths, in which case the spectral index in the IR is ∼0.9, decreasing to ∼0.6 in the radio range (clumped wind Model II). Although this reproduces the observed spectral indices for some WR stars, in other cases (e.g. WR 1, WR 110, WR 147) α increases from the IR–mm to the mm–cm range, indicating an interaction between clumps and interclump medium. A likely explanation for this is the formation of a highly ionized zone, caused by shocks in the outer wind (≥30–100 R_*), the extent of which depends on the optical depth of the outer layers. We shall now elaborate on this in the following section.

4. A high ionization zone in the outer winds of WR stars?

4.1. Formulation of empirical relationship between mass-loss and optical line strength

In general, the observed IR-cm spectral energy distribution of WR winds cannot be reproduced using either a smooth or clumpy wind, under the assumption of constant ionization in this region. We now use an empirical approach to determine the influence of such a high ionization zone on mass-loss rates derived from IR-radio observations.

We wish to determine whether this zone extends beyond the formation region of the cm-fluxes, which is necessary for mass-loss determinations. However, in many cases available data prevents a definitive determination of these radii. Consequently, due to the uncertain radio region ionization state, mass-loss rates suffer from a factor of three uncertainty. We have therefore developed an empirical relationship, based on the assumption that optical emission lines provide relative mass-loss rate estimates, as discussed below.

Let us first assume that $r_{\rm min}$ and $r_{\rm max}$ are the inner and outer radii over which such a high ionization zone extends. For clumped winds in the asymptotic regime, the optical depth $\tau_\nu(\xi)$ (Eq. 16) can then be split into separate integrals:

$$\tau_\nu\ (\xi) = \frac{\dot{M}^2 k_\nu^\circ}{(4\pi\mu m_u v_\infty)^2}\left(\int_\xi^{r_{\rm min}} \frac{\gamma\zeta\delta_{\rm asym} r_{\rm asym} dr}{r^4\sqrt{r^2-\xi^2}} + \right. \quad (21)$$

$$+ \int_\xi^{r_{\rm min}} \frac{\gamma\zeta(1-\delta_{\rm asym})^2 dr}{r^3(1-\delta)\sqrt{r^2-\xi^2}} + \int_{r_{\rm min}}^{r_{\rm max}} \frac{\gamma\zeta\delta_{\rm asym} r_{\rm asym} dr}{r^4\sqrt{r^2-\xi^2}} +$$

$$+ \int_{r_{\rm min}}^{r_{\rm max}} \frac{\gamma\zeta(1-\delta_{\rm asym})^2 dr}{r^3(1-\delta)\sqrt{r^2-\xi^2}} + \int_{r_{\rm max}}^{r_{\rm asym}} \frac{\gamma\zeta\delta_{\rm asym} r_{\rm asym} dr}{r^4\sqrt{r^2-\xi^2}} +$$

$$\left. + \int_{r_{\rm max}}^{r_{\rm asym}} \frac{\gamma\zeta(1-\delta_{\rm asym})^2 dr}{r^3(1-\delta)\sqrt{r^2-\xi^2}} + \int_{r_{\rm asym}}^\infty \frac{\gamma\zeta dr}{r^3\sqrt{r^2-\xi^2}}\right).$$

while f_ν is given by Eq. (17), where the impact parameter ξ_c obeys $\tau_\nu(\xi_c)$=3, $\tau_{r_{\rm asym}}$ is found from Eq. (2) and $\langle\tau_{r_{\rm asym}}\rangle$ is obtained from Eq. (8). In general, we therefore have five unknown parameters, $r_{\rm asym}$, $r_{\rm min}$, $r_{\rm max}$, $\delta_{\rm asym}$ and $\dot{M}$, with other variables, such as d, v_∞, T_e given in Table 2. For cases where the spectral index changes smoothly over the whole IR-radio range we have only three parameters since $r_{\rm min}$ = ∞, and $\tau_\nu(\xi)$ can be found from Eq. (16).

Following the nomenclature of Nugis & Niedzielski (1995), the energy emitted in the line in the clumped case is

$$E_{ki} = \int_V f_c\left(\delta I_{ki}^h + (1-\delta) I_{ki}^l\right)(1-W) dV, \quad (22)$$

where

$$I_{ki}^h(r) = N_k^h \beta_{ik}^h A_{ki} h\nu_{ik}\ , \quad I_{ki}^l(r) = N_k^l \beta_{ik}^l A_{ki} h\nu_{ik}.$$

Here, the terms with subscripts h and l denote the contributions from clumps and the interclump medium, respectively. Using the mass-loss rate formula (Eq. 13), we can express E_{ki} as follows

$$E_{ki} = \frac{\dot{M}^2 A_{ki} h\nu_{ik}}{4\pi R_*(\mu m_u v_\infty)^2}(e_h + e_l), \quad (23)$$

Table 5. The constants c_λ to be used in Eq. (25) for the determination of mass-loss rate using observed optical line equivalent widths

Sp.Type	λ5411 He II	λ4945 N V	λ7115 N IV
WN3	3.3×10^{-11}	4.2×10^{-11}	2.0×10^{-11}
WN4–5	4.8×10^{-11}	9.9×10^{-11}	2.7×10^{-11}
WN4b	5.0×10^{-11}	1.4×10^{-10}	3.1×10^{-11}
WN6/6b	1.2×10^{-10}	2.7×10^{-10}	6.9×10^{-11}
WN7	1.4×10^{-10}		9.3×10^{-11}
WN8	2.5×10^{-10}		2.2×10^{-10}
	λ5411 He II	λ5471 C IV	λ5590 O V
WC5	3.0×10^{-11}	2.5×10^{-11}	2.0×10^{-11}
WC6	3.4×10^{-11}	3.5×10^{-11}	3.6×10^{-11}
WC7	5.4×10^{-11}	4.7×10^{-11}	4.8×10^{-11}
WC8	7.1×10^{-11}	7.0×10^{-11}	9.5×10^{-11}
WC9	1.7×10^{-10}	1.8×10^{-10}	2.2×10^{-10}

where

$$e_h = \int_1^\infty \frac{[\gamma x^+ z_k \beta_{ik}]_h p^2 \delta(1-W) dr'}{[v' r'(p\delta+1-\delta)]^2}, \quad (24)$$
$$e_l = \int_1^\infty \frac{[\gamma x^+ z_k \beta_{ik}]_l (1-\delta)(1-W) dr'}{[v' r'(p\delta+1-\delta)]^2}.$$

In this formulation, $z_k = N_k/N_e N^+$, $x^+ = N^+/N_t$, $r' = r/R_*$ and $v' = v/v_\infty$ (N^+ is the number of atoms in the ionization stage above N_k).

We now assume that stars of the same spectral type have comparable values of $(e_h + e_l)$ for high excitation lines. These lines are formed very close to the stellar surface, where the influence of the clumped structure on the line fluxes is minimal. Assuming that emergent and relative optical fluxes are fairly constant within each spectral type, we obtain our final expression for the mass-loss rate:

$$\dot{M} = c_\lambda \sqrt{W_\lambda} d^{1.5} v_\infty f_v^{0.75} L_W^{0.25} \mu\gamma^{-0.5}, \quad (25)$$

where d is in kpc, v_∞ is in km s^{-1}, $f_v = f_\nu(\mathrm{v})$ is in Jy, $\dot{M}$ is in M$_\odot$ yr^{-1} and c_λ is a numerical constant which will be determined in the following subsection.

4.2. Determination of ionization and clumping-corrected radio mass-loss rates

We have obtained clumping-corrected "radio" mass-loss rates by the following scheme. First we studied stars with many observed flux points covering the whole IR–mm–cm wavelength range, starting by assuming the normal (low) ionization state in the cm forming region. $\dot{M}$, $r_{\rm asym}$ and $\delta_{\rm asym}$ were adjusted to match observations, where we imposed the smooth wind solution as an upper limit to the mass-loss rate. In addition, the maximum value of the filling factor, $\delta_{\rm asym}$ (at $r_{\rm asym}$) cannot exceed ∼2/3 since this corresponds to the maximum filling factor of a spherical shell filled by equal size spherical clumps with diameters equal to the thickness of the shell. $r_{\rm asym}$ can also be constrained from the fact that large matter contrasts are not observed in WR winds; an upper limit of 10^3 was found observationally by Brown et al. (1995) which we adhere to here.

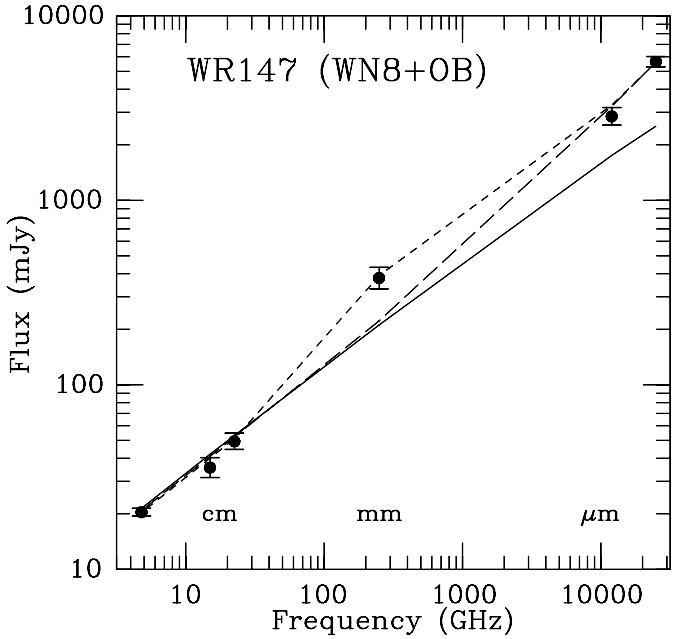

Fig. 3. The observed IR/radio continuum distribution of WR 147 compared to the predictions of smooth and clumped wind models. Smooth wind and constant EF clumped wind models (which produce equal predictions – solid line) and noninteracting type II clumped wind models (long dashes) disagree with the observed continuum distribution, indicated by dots, in contrast with the interacting type II clumped wind model (short dashes) with a "nhn" ionization structure

In the present study we further introduce the parameter $\xi_c^\circ(\lambda_{\max})$, which corresponds to the value of the impact parameter predicted at $\tau_c = 3$ for the longest observed wavelength for a smooth wind (Eq. 9). Since the radio continuum formation zone lies ∼100 times further from the stellar surface than the IR formation zone we set $10\xi_c^0(\lambda_{\max})$ as an upper limit for $r_{\rm asym}$. (The maximum density contrast (10^3) is achieved where IR fluxes are formed, and the density contrast decreases to unity at 10^3 times larger radius).

We investigated alternative solutions depending on the extent of the high ionization zone:

- "nh" in the case where the high ionization zone ends beyond the radio continuum formation zone ($\xi_c(\mathrm{IR}) < \mathrm{r}_{\min} < \xi_c^0(\lambda_{\max})$ and $r_{\max} = \infty$),
- "nhn" where the high ionization zone ends between the IR and radio continuum formation zones ($\xi_c(IR) < r_{\min} < \xi_c^0(\lambda_{\max})$, $r_{\min} < r_{\max} \leq \xi_c^0(\lambda_{\max})$).

Figs. 3–4 demonstrate solutions to the radio ionization state for WR 147 (WN8+OB) and WR 134 (WN6b). Unfortunately, unique solutions were possible for only a few cases. For WR 11 (WC8+O 9) only interacting wind models agree with observation, but the IR/radio data alone are insufficient to distinguish

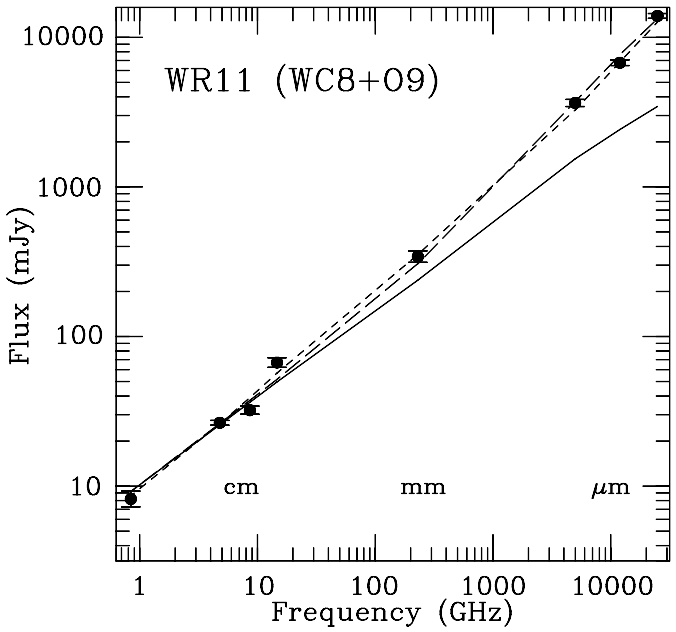

Fig. 4. The observed IR/radio continuum distribution of WR 134 compared with model predictions. Models are as for Fig. 3, with an interacting type II clumped wind model (short dashes, "nhn" ionization structure) required to reproduce observations

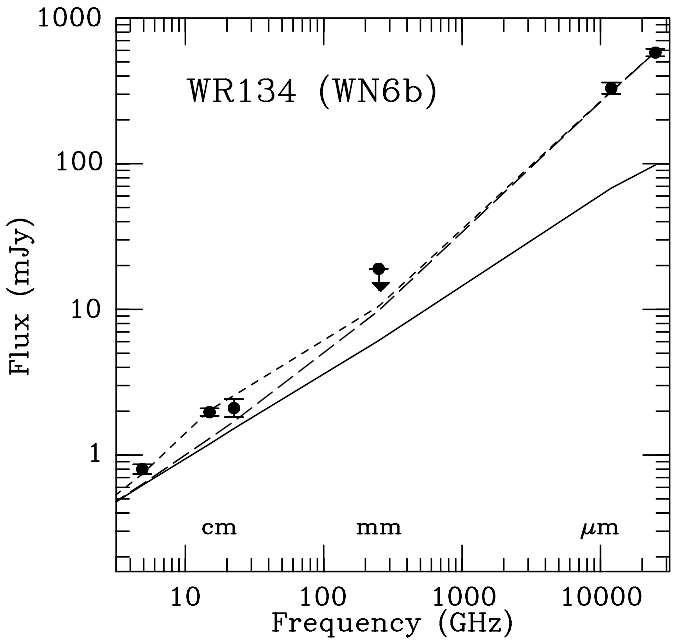

Fig. 5. The observed IR/radio continuum distribution of WR 11 compared with model predictions. Models are as for Fig. 3, with less definitive conclusions. Both interacting type II clumped wind models with "nh" (short dashes) and "nhn" (not shown for clarity) ionization structures are consistent with observations (see Sect. 4.2)

between "nh" and "nhn" solutions (see Fig. 5). In general, IR-radio observations prevented us from distinguishing between the three possibilities. Of these, "n" and "nhn" produced almost identical mass-loss rates, with "nh" solutions yielding mass-loss rates a factor of three lower.

Table 6. Mass-loss rates of WR stars derived from radio–fluxes via the asymptotic clumped wind model, $\dot{M}_{\rm clumped}$, indicating the ionization state (normal, "n", or high, "h") in the cm radio emission zone. For comparison we give mass-loss rates obtained from ≈6 cm radio observations using the smooth wind relationship, $\dot{M}_{\rm smooth}$. Two different smooth wind mass-loss rates are given for WR 89 based on the observations of (1)-Leitherer et al. (1995) and (2)-Abbott et al. (1986)

WR	Sp Type	$\dot{M}_{\rm clumped}$ 10^{-5} M$_\odot$ yr^{-1}	$\dot{M}_{\rm smooth}$ 10^{-5} M$_\odot$ yr^{-1}
1	WN4b	2.40 (h)	6.31
6	WN4b	1.90 (h)	4.82
133	WN5 + O 9I	0.65 (h)	1.81
138	WN5 + B?	1.00 (h)	1.94
139	WN5 + O 6V	0.92 (n)	0.93
141	WN5 + OB?	1.20 (h)	3.01
110	WN5-6b	6.60 (n)	6.71
24	WN6a	2.95 (h)	2.61
25	WN6a	2.90 (h)	4.01
115	WN6	2.35 (n)	2.41
134	WN6b	4.55 (n)	5.54
136	WN6b	6.25 (n)	6.26
22	WN7 + OB	3.40 (h)	5.60
78	WN7	3.80 (n)	3.82
145	WN7/CE + OB?	4.35 (n)	4.32
16	WN8	2.30 (h)	3.80
40	WN8	3.40 (h)	6.63
89[1]	WN8 + abs	5.70 (h)	10.2
89[2]			4.20
98	WN8/C7	5.30 (n)	5.54
147	WN8 + OB	5.30 (n)	5.32
144	WC4	1.10 (h)	2.93
9	WC5 + O 7	2.30 (h)	4.56
111	WC5	1.00 (h)	2.85
15	WC6	1.20 (h)	2.71
146	WC6	1.70 (n)	1.86
79	WC7 + O 5-8	2.40 (h)	6.78
86	WC7 + B 0I	1.70 (h)	4.70
93	WC7 + O 7-9	2.50 (h)	6.71
137	WC7 + OB	2.95 (n)	3.04
140	WC7 + O 4-5	6.30 (n)	6.04
11	WC8 + O 9	1.08 (h)	3.06
113	WC8 + O 8-9IV	3.60: (n)	3.72:
135	WC8	1.50 (h)	4.00
65	WC9	1.50 (n)	1.66
81	WC9	1.60 (n)	1.68
103	WC9	2.40 (n)	2.48
112	WC9	1.10 (n)	1.32

For us to obtain mass-loss rate estimates from radio observations we need to estimate the ionization state where the cm-radio continuuum is formed. We proceeded as follows. Primary standards were adopted for each subclass where a unique cm solution was obtained (namely WR 134, WR 147, WR 113 plus all WC9 stars). Stars with variable radio fluxes (e.g. WR 89) were interpreted as oscillating between a high and low cm-ionization regime. For these primary standards we then obtained coeffi-

cients c_λ that reproduced the derived mass-loss rates for individual optical lines (Eq. 25). Since many subclasses were without suitable standards (WN3–5 and WC4–7), it was necessary to make two further assumptions for the coefficients c_λ: (i) they are comparable within each WR spectral class and (ii) they change smoothly between spectral classes. Depending on the outer ionization balance, two alternative mass-loss rates were obtained from cm fluxes for each star, which could be compared to results from optical lines (Eq. 25). With the above assumptions, we were able to identify mean coefficients c_λ for each WR spectral class. These are presented in Table 5, based on stars with thermal radio emission, plus three additional WN3–4 stars, namely WR 127 (WN3b+O9.5 V) from Sect. 5, and WR 128 (WN4) and WR 3 (WN3b+O4) using (clumping-corrected) mass-loss rates derived by Nugis & Niedzielski (1995) from an optical-IR analysis. For individual stars without radio fluxes, the ionization state in the radio emission zone follows from c_λ, which allows mass-loss rate predictions using the empirical formula (Eq. 25). In the following section we present our clumping-corrected WR mass-loss rates, and compare these with estimates obtained from independent techniques.

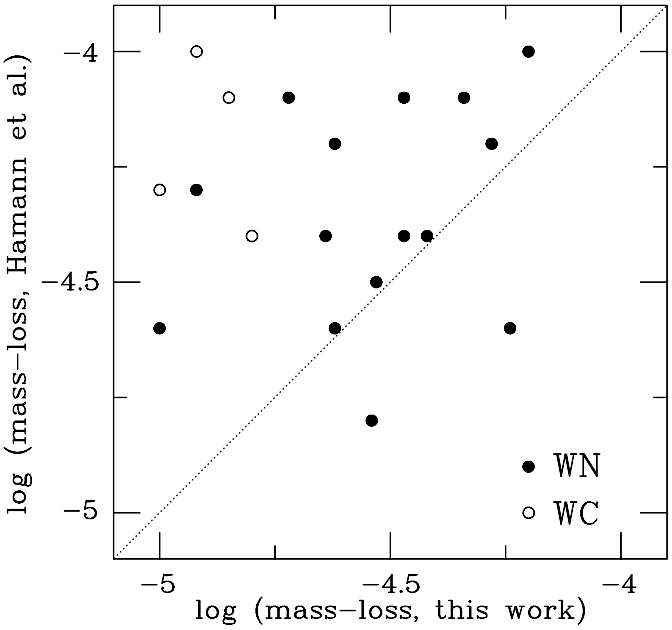

Fig. 6. Comparison between WR mass-loss rates (in $M_\odot \mathrm{yr}^{-1}$) obtained here for single stars, with those derived from non-LTE modelling of optical recombination lines assuming a smooth wind by Hamann et al. (1995) for WN stars (dots) and Koesterke & Hamann (1995) for WC stars (open circles)

5. Derived mass-loss rates and comparison with other results

Table 6 presents clumping-corrected "radio" mass-loss rates, including smooth wind results for comparison. Major differences between mass-loss rates from clumped and smooth models are exclusive to the models with a "nh" ionization structure. In some stars the extent of the highly ionized zone may be time variable. This may explain changes in radio emission in WR 89 and WR 11 (probably also WR 22 and WR 24) as indicated by their unusual spectral indices.

The majority of mass-loss rate determinations for WR stars rely on smooth wind assumptions, either using optical (Hamann et al. 1995, Crowther et al. 1995a) or radio (Abbott et al. 1986, Leitherer et al. 1997) methods. A limited number of studies using clumping-independent techniques have now been carried out.

In the case of single stars, most Galactic WR stars have now been studied using non-LTE model atmospheric analyses of (mostly) optical emission lines under the assumption of smooth winds. Although other groups have carried out such studies, Hamann et al. (1995) and Koesterke & Hamann (1995) have systematically analysed the largest sample of respectively, WN and WC stars. We present a comparison of mass-loss rates derived here with their results in Fig 6, having first corrected previous results to account for our assumed distances. Clearly, we obtain significantly lower mass-loss rates than Hamann et al. (1995) and Koesterke & Hamann (1995) by relaxing their smooth wind assumption. Overall, we obtain $\log \dot{M}$(this work)$-\log \dot{M}$(Hamann et al.)$=-0.19$ (σ=0.28) for 15 WN stars, and $\log \dot{M}$(this work)$-\log \dot{M}$(Koesteke & Hamann)$=-0.62$ (σ=0.19) for 4 WC stars in common.

Schmutz (1997) has recently analysed WR 6 (HD 50896, WN4b) using a non-LTE model atmosphere accounting for clumping. He derived a value of 3.2×10^{-5} $\mathrm{M}_\odot\mathrm{yr}^{-1}$, in reasonable agreement with our value of 1.9×10^{-5} $\mathrm{M}_\odot\mathrm{yr}^{-1}$, and significantly lower than 8×10^{-5} $\mathrm{M}_\odot\mathrm{yr}^{-1}$, derived by Hamann et al. (1995) assuming a smooth outflow.

St-Louis et al. (1988) determined mass-loss rates for ten WR stars in massive binaries using polarization techniques which were independent of clumping and distance. Mass-loss rates derived in this way are sensitive to various parameters (Eq. (6) in St-Louis et al.) which have subsequently been revised and compiled in Table 7. In addition, St-Louis et al. assumed that the WR atmospheres were composed of doubly ionized helium.

Here we correct the mass-loss rates derived by St-Louis et al. (1988) for improved chemical composition and ionization structure. For those WN binaries not studied by Nugis & Niedzielski (1995) we found H/He≈0.2 for WR 139 and WR 47, with H/He≈0.0 for WR 127 and, as before assumed N/He=0.005. For WC components we used abundances compiled in Sect. 2. We assume that the effective region of linear polarization modulation lies beyond $\tau_e \leq 0.2$–0.3 (St-Louis et al. 1988). Estimates of the number of free electrons per ion in the region where electron scattering processes are effective for polarization modulation were estimated from our clumped wind models:

- WN3: $z(\mathrm{He})$=2.0, $z(\mathrm{N})$=5.0,
- WN5: $z(\mathrm{He})$=1.5, $z(\mathrm{N})$=4.0,
- WN6: $z(\mathrm{He})$=1.4, $z(\mathrm{N})$=4.0,
- WN8: $z(\mathrm{He})$=1.1, $z(\mathrm{N})$=3.0,
- WC7: $z(\mathrm{He})$=1.25, $z(\mathrm{C})$=3.0, $z(\mathrm{O})$=4.0,
- WC8: $z(\mathrm{He})$=1.1, $z(\mathrm{C})$=2.5, $z(\mathrm{O})$=3.5.

Table 7. Parameters of binary WR stars studied by St-Louis et al. (1988), including revised polarization mass-loss rates (see text). Distance estimates are obtained from: association or cluster membership (a), absolute visual magnitude (M_v), O star radius ($R_{\rm O}$) or parallax measurements (cf. explanations to the Table 2). We indicate references to sources of parameters v_∞, a, i which differ from those used by St-Louis et al. (1988) in parenthesis. Colons indicate uncertain data

WR		Sp	m_v mag	E_{B-V} mag	L_W	d kpc	M_v mag	a $R_\odot$	i	v_∞ km s^{-1}	$\dot{M}_{\rm pol}$ $10^{-5}M_\odot$ yr^{-1}
127	WN3b	+ O9.5 V	10.33	0.50	0.28 (13)	4.37 (a)	−3.20	67	$55.7^\circ \pm 8.2$	1760 (1)	0.49
133	WN5	+ O9 I	6.70	0.38	0.12	1.66 (a)	−3.40	307 (2)	20°: (3)	1625 (4)	0.65:
139	WN5	+ O6 V	8.10	0.88	0.35	1.13 ($R_{\rm O}$)	−4.04	36.5(5)	$78.7^\circ \pm 0.5$ (6)	1785 (4)	0.84
47	WN6	+ O5 V	11.12	1.22	0.65 (14)	4.30 (ΔM_v)	−5.75	68	$70^\circ \pm 4$ (7)	2460 (1)	7.50
153	WN6/CE	+ O6 I:	9.08	0.65	0.36 (15)	3.47 (a)	−4.74	51	$78.2^\circ \pm 1.0$	1785 (4)	2.50:
148	WN8	+ abs	10.46	0.75	0.66 (16)	7.75 ($M_v^{\rm W}$)	−6.10	41	$66.6^\circ \pm 4$	1545 (11)	4.42:
155	WN6	+ O9	8.74	0.66	0.44 (17)	3.47 (a)	−5.36	19 (8)	$72^\circ \pm 6$ (9)	1690 (4)	3.43:
42	WC7	+ O7 V	8.27	0.37	0.32 (18)	3.02 ($M_v^{\rm O}$)	−4.16	52	$43.5^\circ \pm 3.0$	1645 (4)	1.09
79	WC7	+ O5-8	6.97	0.48	0.45	1.58 (a)	−4.80	69	29.5°: (10)	2270 (4)	3.30
11	WC8	+ O9 III	1.78	0.03	0.15	0.26 (par)	−3.34	240 (12)	$70^\circ \pm 10$	1415 (4)	1.35:

(1)-$v_\infty = 0.74v$(Abbott & Conti 1987), as derived by Willis (1991), (2)-Underhill & Hill (1994), (3)-i is taken from Underhill & Hill (1994) estimate of $M_{\rm W}\sin^3 i$ and Smith et al. (1994) estimate that $M_{\rm W} \approx 10M_\odot$, (4)-Prinja et al. (1990), (5)-Marchenko et al. (1994), (6)-Robert et al. (1990), (7)-Moffat et al. (1990), (8)-Marchenko et al. (1995), (9)-the mean of the estimates of Lipunova & Cherepashchuk (1982) and St-Louis et al. (1988), (10)-i is taken from Seggewiss (1974) assuming an O6.5V mass of 41 $M_\odot$ (Vacca et al. 1996), (11)-Rochowicz & Niedzielski (1995), (12)-Schaerer et al. (1997), (13)-the mean of $L_{\rm abs} \approx 0.23$ (Massey 1981) and $L_{\Delta M_v} \approx 0.32$ expected from components, (14)-the mean of $L_{\rm abs} \approx 0.80$ (Niemela et al. 1980) and $L_{\Delta M_v} \approx 0.49$ expected from components, (15)-$L_{\rm em}$, (16)-the mean of $L_{\rm em} \approx 0.40$ and $L_{\Delta M_v} \approx 0.83$ – Marchenko et al. (1996), (17)-the mean of $L_{\rm em} \approx 0.30$ and $L_{\rm abs} \approx 0.57$ (Marchenko et al. 1995), (18)-$L_{\rm em}$

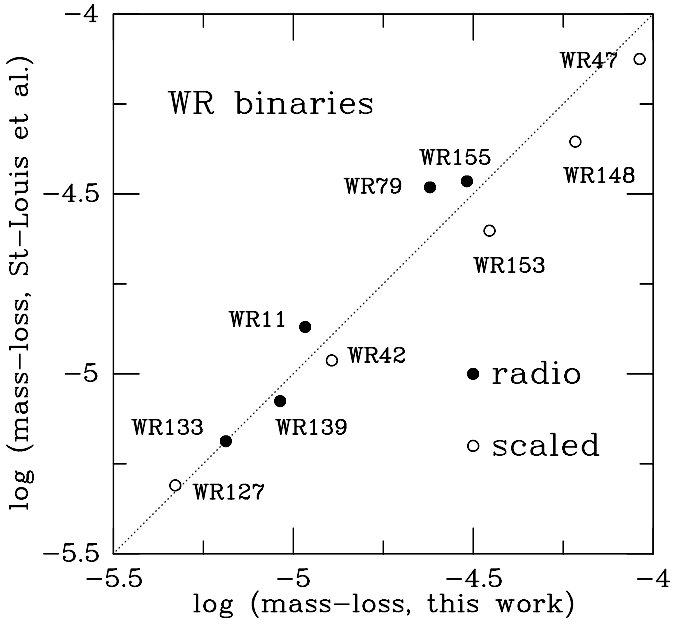

Fig. 7. Comparison between WR binary mass-loss rates (in $M_\odot$yr^{-1}) obtained here with those derived from the clumping independent technique of St-Louis et al. (1988), corrected for revised orbital and stellar parameters. Dots denote stars for which mass-loss rates were directly obtained from radio observations, while open circles denote those stars whose mass-loss rates were obtained using our scaling formulae

Fig. 7 compares (corrected) polarization mass-loss rates with our derived mass-loss rates, demonstrating the excellent agreement between the two methods, even for cases in which binary properties are relatively poorly constrained.

Several independent mass-loss rate determinations have been made for WR 139 (V444 Cyg). St-Louis et al. (1993) analyzed its polarization eclipse observations revealing a WN5 component mass-loss rate of 0.62×10^{-5} M$_\odot$ yr^{-1} after correcting for ionization structure and $L_{\rm W}$. This is somewhat lower than that derived from the polarization amplitude and IR-radio continuum fluxes. Khaliullin et al. (1984) have found that the period of this system is increasing at the rate 0.202 ± 0.018 s yr^{-1} which assuming masses and inclinations from Marchenko et al. (1994) and Robert et al. (1990) implies $\dot{M} = (1.03\pm0.13)\times10^{-5}M_\odot$ yr^{-1}, in very good accord with our derived value. However, using the revised rate of increase in period of Underhill et al. (1990), a substantially lower $\dot{M} = (0.45 \pm 0.13) \times 10^{-5}M_\odot$ yr^{-1} is obtained. Clearly, new studies are urgently needed to clarify this situation for this star.

In conclusion, we have utilised IR–radio continuum fluxes to constrain the ionization structure and clumped nature of the outer winds of WR stars. Observed WR spectral indices can be explained by clumped wind models in which shocks between clumps (at about a hundred stellar radii) produce a higher ionization zone, which may extend beyond the radio formation region. Coordinated long-term radio and X-ray observations of WR stars should help to clarify the structure of their outer wind regions. From an empirical formula we obtain WR mass-loss rates which are lower than those obtained from assuming smooth winds, though are in excellent agreement with measurements from clumping independent techniques for WR binaries. In a

future work we will attempt to derive the dependence of mass-loss rates on fundamental stellar parameters.

Acknowledgements. This work was supported by the Estonian Science Foundation grant No. 827. PAC acknowledges financial support from PPARC.

References

Abbott D.C., Conti P.S., 1987, Ann. Rev. A&A 25, 113
Abbott D.C., Bieging J.H., Churchwell E., 1981, ApJ 250, 645
Abbott D.C., Bieging J.H., Churchwell E., Torres A.V., 1986, ApJ 303, 239
Altenhoff W.J., Thum C., Wendker H.J., 1994, A&A 281, 161
Antokhin I.I., Nugis T., Cherepashchuk A.M., 1992, Astron. Zh. 69, 516
Barlow M.J., Smith L.J., Willis A.J., 1981, MNRAS 196, 101
Becker R.H., White R.L., 1985, ApJ 297, 649
Bieging J.H., Abbott D.C., Churchwell E.B., 1982, ApJ 263, 207
Blomme R., Runacres M.C., 1997, A&A 323, 886
Brown J.C., Richardson L.L, Antokhin I., et al., 1995, A&A 295, 725
Carson T.R., 1988, A&A 189, 319
Cherepashchuk A.M., Eaton J.A., Khaliullin Kh.F., 1984, ApJ 281, 774
Cherepashchuk A.M., Koenigsberger G., Marchenko S.V., Moffat A.F.J., 1995 A&A 293, 142
Churchwell E., Bieging J.H., van der Hucht K.A., et al., 1992, ApJ 393, 329
Cohen M., Barlow M.J., Kuhi L.V., 1975, A&A 40, 291
Crawford I.A., Barlow M.J., 1991, A&A 249, 518
Crowther P.A., 1993, PhD Thesis, University of London
Crowther P.A., Hillier D.J., Smith L.J., 1995a, A&A 293, 403
Crowther P.A., Smith L.J., Hillier D.J., Schmutz W., 1995b, A&A 293, 427
Crowther P.A., Smith L.J., Willis A.J., 1995c, A&A 304, 269
Dougherty S.M., Williams P.M., van der Hucht K.A., Bode M.F., Davis R.J., 1996, MNRAS 280, 963
Eaton J.A., Cherepashchuk A.M., Khaliullin Kh.F., 1985, ApJ 296, 222
Eenens P.R.J., Williams P.M., 1994, MNRAS 269, 1082
Felli M., Panagia N., 1982, ApJ 262, 650
Ford G., Stickland D.J., 1988, in "New Insights in Astrophysics", ESA SP 263, p.502
Garmany C.D., Massey P., Conti P.S., 1984, ApJ 278, 233
Hackwell J.A., Gehrz R.D., Smith J.R., 1974, ApJ 192, 383
Hamann W.-R, Schwarz E., 1992, A&A 261, 523
Hamann W.-R, Koesterke L., Wessolowski U., 1995, A&A 299, 151
Hillier D.J., 1989, ApJ 347, 392
Hillier D.J., 1991, A&A 247, 455
Hogg D.E., 1982, in "Wolf-Rayet Stars, Observations, Physics, Evolution", Proc. IAU Symp. 99, eds. C. de Loore, A. J. Willis, Dordrecht, Reidel, p. 221
Hogg D.E., 1989, AJ 98, 282
Howarth I.A., Schmutz W., 1995, A&A 294, 529
van der Hucht K.A., Hidayat B., Admiranto A.G., Supelli K.R., Doom C., 1988, A&A 199, 217
Jones P.A., 1985, MNRAS 216, 613
Khaliullin K.F., Khaliullina A.I., Cherepashchuk A.M., 1984, Soviet Astron. Letters 10, 250
Koesterke L., Hamann W.-R., 1995, A&A 299, 503
Lamers H.J.G.L.M., Waters L.B.F.M., 1984, A&A 138, 25
Leitherer C., Robert C., 1991, ApJ 377, 629
Leitherer C., Chapman J.M., Koribalski B., 1995, ApJ 450, 289
Leitherer C., Chapman J.M., Koribalski B., 1997, ApJ 481, 898
Lipunova N.A., Cherepashchuk A.M., 1982, Soviet Astron. J. 26, 569
Lundström I., Stenholm B., 1984, A&A 58, 163
Marchenko S.V., Moffat A.F.J., Koenigsberger G., 1994, ApJ 422, 810
Marchenko S.V., Moffat A.F.J., Eenens P.R.J., Hill G.M., Grandchamps A., 1995, ApJ 450, 811
Marchenko S.V., Moffat A.F.J., Lamontagne R., Tovmassian G.H., 1996, ApJ 461, 386
Massey P., 1981, ApJ 244, 157
Massey P., 1984, ApJ 281, 789
Massey P., Niemela V.S., 1981, ApJ 245, 195
Moffat A.F.J., Drissen L., Lamontagne R., Robert C., 1988, ApJ 334, 1038
Moffat A.F.J., Drissen L., Robert C., et al., 1990, ApJ 350, 767
Morris P.W., Brownsberger K.R., Conti P.S., Massey P., Vacca W.D., 1993, ApJ 412, 324
Morton D.C., Wright A.E., 1978, MNRAS 182, 47P
Niemela V.S., Conti P.S., Massey P., 1980, ApJ 241, 1050
Nugis T., 1990, Astrophysics 32, 51
Nugis T., 1991, in "Evolution of Stars, the Photospheric Abundance Connection", Proc. IAU Symp. 145, eds. G. Michaud, A. Tutukov, Kluwer, p. 209
Nugis T., 1994, in "Instability and Variability of Hot–Star Winds" (Astrophys. Space Sci. 221), eds. A.F.J. Moffat, S.P. Owocki, A.W. Fullerton, N. St-Louis, Kluwer, p. 217
Nugis T., 1996, in "Wolf–Rayet Stars in the Framework of Stellar Evolution", Proc. 33rd Liège International Astrophysical Colloquim, eds. J.–M. Vreux, A. Detal, D. Fraipont–Caro, E. Gosset, G. Rauw, Kluwer, p. 283
Nugis T., Niedzielski A., 1995, A&A 300, 237
Nussbaumer H., Schmutz W., Smith L.J., Willis A.J., 1982, A&AS 47, 257
Panagia N., Felli M., 1975, A&A 39, 1
Pitault A., Epchtein N., Gómez A., Lortet M.C., 1983, A&A 120, 53
Prinja R.K., Barlow M.J., Howarth I.D., 1990, ApJ 361, 607
Rauw G., Vreux J.-M., Gosset E., et al., 1996, A&A 306, 771
Robert C., 1994, in "Instability and Variability of Hot–Star Winds" (Astrophys. Space Sci. 221), eds. A.F.J. Moffat, S.P. Owocki, A.W. Fullerton, N. St-Louis, Kluwer (Astrophys. Space Sci. 221), p.137
Robert C., Moffat A.F.J., Bastien P., St-Louis N., Drissen L., 1990, ApJ 359, 211
Rochowicz K., Niedzielski A., 1995, Acta Astronomica 45, 307
Runacres M.C., Blomme R., 1996, A&A 309, 544
Schaerer D., Schmutz W., Grenon M., 1997, ApJ 484, L153
Schmutz W., 1997, A&A 321, 268
Schmutz W., Vacca W.D., 1991, A&AS 89, 259
Seggewiss W., 1974, A&A 31, 211
Smith L.F., 1968, MNRAS 140, 409
Smith L.F., Maeder A., 1989, A&A 211, 71
Smith L.F., Shara M.M., Moffat A.F.J., 1990, ApJ 358, 229
Smith L.F., Meynet G., Mermilliod J.-C., 1994, A&A 287, 835
Smith L.F., Shara M.M., Moffat A.F.J., 1996, MNRAS 281, 163
Stickland D.J., Bromage G.E., Budding E., et al., 1984, A&A 134, 45
St-Louis N., Moffat A.F.J., Drissen L., Bastien P., Robert C., 1988, ApJ 330, 289
St-Louis N., Moffat A.F.J., Lapointe L., et al., 1993, ApJ 410, 342
Torres A.V., 1985, PhD Thesis, JILA, Colorado
Torres-Dodgen A.V., Massey P., 1988, AJ 96, 1076
Turner D.G., 1982, in "Wolf-Rayet Stars, Observations, Physics, Evolution", Proc. IAU Symp. 99, eds. C. de Loore, A. J. Willis, Dordrecht, Reidel, p. 57

Underhill A.B., 1983, ApJ 266, 718
Underhill A.B., Hill G.M., 1994, ApJ 432, 770
Underhill A.B., Grieve G.R., Louth H., 1990, PASP 102, 749
Vacca W.D., Torres-Dodgen A.V., 1990, ApJS 73, 685
Vacca W.D., Garmany D.C., Shull J.M., 1996, ApJ 460, 914
Williams P.M., Antolopoulou E., 1981,MNRAS 196, 915
Williams P.M., Longmore A.J., van der Hucht K.A., et al., 1985, MNRAS 215, 23P
Williams P.M., van der Hucht K.A., Thé P.S., 1987, A&A 182, 91
Williams P.M., van der Hucht K.A., Pollock A.M.T., et al., 1990, MNRAS 243, 662
Williams P.M., Dougherty S.M., Davis R.J., et al., 1997, MNRAS 289, 10
Willis A.J., 1991, in “Wolf-Rayet Stars and Interrelations with Other Massive Stars in Galaxies”, Proc. IAU Symp. 143, eds. K.A. van der Hucht, B. Hidayat, Kluwer, p. 265
Willis A.J., Dessart L., Crowther P.A., et al., 1997, MNRAS 290, 371
Wright A.E., Barlow M.J., 1975, MNRAS 170, 41